

Functional Characterization of Cinnamyl Alcohol Dehydrogenase during Developmental Stages and under Various Stress Conditions in Kenaf (*Hibiscus cannabinus* L.)

Bosung Choi,^a Jun Y. Chung,^b Hyeun-Jong Bae,^c Inhwan Bae,^{d,*} Seonjoo Park,^{e,*} and Hanhong Bae^{a,*}

In this study, the entire gene encoding cinnamyl alcohol dehydrogenase in kenaf (*HcCAD2*) was cloned and characterized. CAD is a key enzyme in the last step of lignin biosynthesis. The full-length *HcCAD* ortholog is composed of a 1,074-bp open reading frame (ORF) encoding 357 amino acids (KM044582). BlastP and a phylogenetic study revealed that the deduced amino acid sequences share the highest similarity with *Gossypium hirsutum* (ABZ01817) (89%). Upon real-time PCR analysis, *HcCAD1* (HM151380) and *HcCAD2* were highly up-regulated in 4-week-old stem and mature flower tissues, which was matched with histochemical staining and lignin component analysis. The expression patterns of the two genes differed in response to wound, cold, NaCl, SA, H₂O₂, ABA, MeJA, and drought. CAD enzyme activity was measured with various aldehydes as substrates to form corresponding alcohols. The results indicated that the preferred substrates were coniferyl and sinapyl aldehydes with high catalytic efficiency.

Keywords: Cinnamyl alcohol dehydrogenase (CAD); Abiotic stress; Enzyme assay; Real-time PCR; Lignin

Contact information: a: School of Biotechnology, Yeungnam University, Gyeongsan, Gyeongbuk 712-749, Republic of Korea; b: Department of Orthopedic Surgery, School of Medicine, Ajou University, Suwon 442-749, Republic of Korea; c: Department of Bioenergy Science and Technology, Chonnam National University, Gwangju 500-757, Republic of Korea; d: College of Pharmacy, Chungang University, Seoul 156-756, Republic of Korea; e: Department of Life Sciences, Yeungnam University, Gyeongsan, Gyeongbuk 712-749, Republic of Korea;

* Corresponding authors: inhwan.bae@gmail.com; sjpark01@ynu.ac.kr; hanhongbae@ynu.ac.kr

INTRODUCTION

Kenaf (*Hibiscus cannabinus* L.), an annual dicotyledonous plant, thrives in various habitats ranging from temperate to tropical regions, including arid areas (Dempsey 1975). Because kenaf has a high growth rate and broad ecological adaptability, it is believed to have great potential as a source for future biomass production. Kenaf has also been used for pulp and paper production because of its high quality fiber (Pande and Roy 1996). Because the bark of kenaf accounts for 35% to 40% of its total stem weight and its stems are composed of relatively long outer fibers and short inner fibers at a 1:3 ratio, its fibers are a promising raw material for use by the pulp industry. During pulping, lignin increases costs and reduces the efficiency of the process. Additionally, the accessibility of microbial, cell wall-degrading enzymes is reduced by the protection of cell wall polysaccharides by lignin. Recent studies have been conducted to develop genetically modified plants with lower lignin contents or different compositions. Kenaf contains less than 11% lignin and

more cellulose than other non-woody plants (Gutiérrez *et al.* 2004). High levels of polysaccharides are not only beneficial to pulping, but also provide a great advantage to bioethanol production. In addition, the fibers have a high proportion of S units of lignin, which are more easily digestible than other lignin units (G and H units) (Gutiérrez *et al.* 2004).

Lignin biosynthesis is conducted *via* the phenylpropanoid pathway, which is divided into two major steps: monolignol biosynthesis (coniferyl, sinapyl, and p -coumaryl alcohols) and cross-linkage of monolignols by peroxidase and laccase enzymes. In monolignol biosynthesis, a series of enzymatic reactions is carried out by 10 distinct enzymes. The initial step is carried out by phenylalanine ammonia lyase (PAL), which is catalyzed by cinnamyl alcohol dehydrogenase (CAD) and deaminates phenylalanine, forming coniferyl, sinapyl, and p -coumaryl alcohols. CAD converts cinnamyl aldehyde to cinnamyl alcohol in the final step of the pathway and is therefore a key enzyme in monolignol biosynthesis. In gymnosperms, CAD is usually encoded by one gene with high activity for the reduction of coniferyl aldehyde, but not for sinapyl aldehyde (Galliano *et al.* 1993). Conversely, CAD in angiosperms is usually encoded by multiple genes with high specificity to both coniferyl and sinapyl aldehydes (Brill *et al.* 1999). In Arabidopsis, CAD consists of nine genes (AtCAD1 to AtCAD9), but only AtCAD1, AtCAD4, and AtCAD5 play important roles in lignin biosynthesis (Kim *et al.* 2004). Deficiencies in each gene are known to result in reduced lignin content and compounds. Down-regulation of CAD expression in poplar and tobacco led to enhanced levels of coniferyl and sinapyl aldehydes (Ralph *et al.* 2001), and it was easier to remove lignin from the poplar and tobacco plants subjected to CAD down-regulation. In addition, more free phenolic groups could be generated because of the increased alkaline solubility of the lignin and thus, the pulping efficiency (Lapierre *et al.* 2004).

In this study, the function and expression patterns of CAD during different developmental stages and under various stress conditions were characterized. The results presented in this study provide information that will lead to improved biomass properties in materials used by the pulp and bioethanol industries.

EXPERIMENTAL

Plant Materials

Kenaf seeds (*Hibiscus cannabinus* L., C-9) produced by the Advanced Radiation Technology Institute (Korea Atomic Energy Research Institute, Jeongseup 580-185, Korea) were sown in a flat system composed of 32 individual pots containing a non-soil mixture (TOBIETEC). The growth room conditions were as follows: 16-h light/8-h dark photoperiod; 22 °C; and 100 $\mu\text{mol}/\text{m}^2/\text{s}$ light intensity for four weeks. Four-week-old plants were transferred into 20-cm pots with a non-soil mixture and grown in a greenhouse under natural sunlight for up to 20 weeks with watering twice a week. Samples for tissue-specific analysis (roots, stems, petioles, leaves, and flowers) were collected from 16-week-old plants. Three-week-old seedlings were used for various stress treatments. The treatments were as previously described (Choi *et al.* 2012).

CAD Cloning

RNA extraction was conducted as previously described (Choi *et al.* 2012). Degenerate primer sequences were designed based on the consensus sequences of the CAD

orthologs of *Populus trichocarpa* (EU603306), *Gossypium hirsutum* (EU857624), *Solanum lycopersicum* (AK323694), *Linum album* (AJ811963), and *Arabidopsis thaliana* (NM119587). The forward and reverse primers were as follows: forward primer (*CAD-F*), 5'-CCTGG(C/G/A)CA(T/C)GAAGT-3'; and reverse primer (*CAD-R*), 5'-TCCTC(C/T)GT(T/C)TCCTTCAT-3'. Amplified products were purified using a Wizard SV Gel and a PCR Clean-up System (Promega) and were then inserted into the pGEM-T easy Vector (Promega). DNA sequencing was carried out by Cosmogenetech Co. To complete the cloning of the full-length kenaf *CAD* ortholog, both 5' and 3' RACE (rapid amplification of cDNA ends) were conducted according to the manufacturer's guidelines (Invitrogen). Two sets of gene specific primers (GSP) were used for 5' RACE: 5'GSP3, 5'-CTGCAACATCCAACAAGACA-3'; 5'GSP2, 5'-CGTTGTACGACCAGATCTTC-3'; and 5'GSP1, 5'-ATGCTCCAATGCCTCGACTT-3'. The following primers were used for 3' RACE: 3'GSP1, 5'-AAGTCGAGGCATTGGAGCAT-3'; 3'GSP2, 5'-ACTCGATTACATCATCGACA-3'; and 3'GSP3, 5'-CTCTCGAGCCTTACCTTTC-3'. The full length of the *HcCAD2* gene was amplified using the forward and reverse primers with BamHI and HindIII sites added as follows: forward primer, 5'-GGCCGGATCCATGGGTAGCCTTGAAACC-3'; and reverse primer, 5'-GGCCAAGCTTTGGATCGAGCTTGCTTCC-3'. Validation of the amplified product was confirmed by sequencing. Finally, the samples were digested with restriction enzymes and the products were cloned into the same sites of the pET-28a vector (Novagen).

Quantitative Real-Time Reverse Transcription PCR (QPCR) Analysis

QPCR was conducted as previously described by Bae *et al.* (2008) using an Mx3000P QPCR System (Agilent) with SYBR Green QPCR Master Mix (LPS Solution). Primer 3 software of the Biology Workbench (<http://workbench.sdsc.edu/>) was applied to design primers for *HcCAD1* and *HcCAD2*. Primer specificity was validated using a dissociation curve. The forward and reverse primers of the *HcCAD* orthologs were as follows: *HcCAD1* forward primer, 5'-CTTACCTTTCGTTGCTGAGACAT-3'; *HcCAD1* reverse primer, 5'-GATATAATCCATCTTCACCACTTCG-3'; *HcCAD2* forward primer, 5'-AGGAAATCACAGGGAGTTTCATTG-3'; and *HcCAD2* reverse primer, 5'-CCACTTAATCTATGGATCGAGCTT-3'. ACTIN (DQ866836), a housekeeping gene, was analyzed for expression normalization using the following primers: *HcACT* forward primer, 5'-AAGTTCTCGAACGAGAAGCTGAT-3'; and *HcACT* reverse primer, 5'-AGTGATTTCTTGCTCATAACGGT-3'. Validation of the amplified products was confirmed by sequencing. Average values were calculated from three biological replications.

Data Analysis

Analysis of DNA and protein sequences was performed using NCBI Blast (<http://blast.ncbi.nlm.nih.gov/>), Biology WorkBench (ClustalW), the ExPASy Proteomics Server (<http://expasy.org/tools/pitool.html>), Superfamily 1.75 (<http://supfam.org/SUPERFAMILY/index.html>), SignalP 3.0 (<http://www.cbs.dtu.dk/services/SignalP/>), and TargetP V1.1 (<http://www.cbs.dtu.dk/services/TargetP/>). A phylogenetic tree was constructed using the neighbor joining method in Mega5 (<http://www.megasoftware.net>). Student's t-test and Duncan multiple range test (SAS, SAS Institute Inc. Korea) were performed to determine the statistical significance.

CAD Enzyme Kinetic Assay

The pET-28a-HcCAD2 vector was introduced into *E. coli* (BL21), which was incubated at 37 °C in Luria-Bertani (LB) medium containing 2 mM ZnCl₂ and 50 mM Kanamycin until the OD₆₀₀ reached 0.8. Next, 1 mM IPTG was added into the LB medium and the cells were grown at 18 °C for 16 h. The cells were subsequently harvested by centrifugation at 5,000 g for 30 min, after which the aqueous phase was removed and the cells were resuspended in lysis buffer (100 mM Tris-HCl, pH 8.0; 300 mM NaCl; 10 mM imidazole) and then incubated with lysozyme (final concentration of 2 mg/mL) on ice for 1 h. Following sonication, cell lysates were precipitated by centrifugation at 5,000 g for 30 min. Next, the recombinant proteins in the supernatant were purified using a Ni-NTA His-Bind Resin (BioRad) according to the manufacturer's instructions. Finally, the protein concentration was determined by Bradford assay using spectrophotometry. The enzyme activity of HcCAD2 was determined according to the modified method described by Ma (2010). In every reaction, automatic observation for declination at OD₃₄₀ was carried out in 1-min intervals for 10 min. Extrapolation from Lineweaver-Burke plots was then used to calculate K_m and V_{max} . Additionally, the influence of the pH on the enzyme activity was examined by adding the reaction mixture to sodium phosphate buffers of various pH values for 15 min. To measure the enzyme stability, the enzyme activity was measured after incubation of the reaction mixture at different temperatures. The final reaction mixture consisted of 100 mM sodium phosphate buffer (pH 6.0), 34 μM aldehyde, 100 μL of enzyme, and 100 μM NADPH. This experiment was performed three times.

Histochemistry of Lignin Deposition

To observe the lignin distribution, kenaf stems from each developmental stage were cut into uniform sections using a razor blade and stained with phloroglucinol (2% w/v phloroglucinol acidified in 6 M HCl) for 30 s. After staining, the samples were placed in glycerol and observed under a light microscope (Olympus BX51) equipped with a digital camera.

Lignin Content and Component Analysis

Kenaf samples were ground in a Wiley mill to obtain 40- to 60-mesh meal which was then Soxhlet-extracted with a mixture of alcohol and benzene (1:2) until the solvent was clear of any color. The extract content was then determined as described by TAPPI methods (TAPPI 1992), after which the lignin monomers were determined by nitrobenzene oxidation (Chen 1992). Next, extractive-free samples of about 20 to 30 mg weight were reacted with 4 mL of 2 N NaOH solution and 0.25 mL of nitrobenzene oxidant in a stainless steel vessel for 2 h at 170 °C in a heating block. The reaction mixture was then cooled on ice and mixed with 0.1 mL of dichloromethane containing 5 mg of 3-ethoxy-4-hydroxybenzaldehyde as an internal standard. The oxidation mixture was then transferred to a liquid-liquid extractor and extracted three times with 30 mL of dichloromethane to remove the nitrobenzene reduction products and any excess nitrobenzene. The aqueous layer was subsequently acidified to pH 1 to 2 with 4 M HCl solution, after which it was further extracted twice with 30 mL of dichloromethane and once with ethyl ether, dried over Na₂SO₄, and evaporated to dryness at reduced pressure. The dried products were dissolved in 0.1 mL of N-(trimethylsilyl) acetamide and analyzed by gas chromatography (Chrompack CP-9100, Agilent) using a CP-Sil 5 CB fused silica capillary column (25 m × 0.32 mm i.d., 1.2 μm film thickness). The operating conditions were as follows: detector temperature, 280 °C; injector temperature, 280 °C; and oven temperature programmed to

rise from 150 (5 min) to 250 °C at 10 °C /min. There were four biological replications of this experiment.

Sugar Analysis

Monosaccharides were measured in the kenaf stem tissues (4- and 12-week-old) using gas chromatography (GC-2010; Shimadzu) according to the method described by Wi *et al.* (2009). The stem tissues were hydrolyzed with 72% sulfuric acid at room temperature for 45 min, after which the samples were diluted with water to 4% sulfuric acid concentration and autoclaved at 121 °C for 1 h. The samples were then neutralized by adjusting the pH to 7.0 with ammonia. Myo-inositol was used as an internal standard. After adding dimethyl sulfoxide (0.1 mL) containing 2% sodium tetrahydroborate (NaBH₄), the samples were incubated at 70 °C for 30 min. To decompose the sodium tetrahydroborate, 0.1 mL of acetic acid (18 M) was added. To enable complete acetylation, 0.2 mL of methylimidazol and 2 mL of anhydrous acetic acid were added and the samples were mixed vigorously and incubated at room temperature for 10 min. Next, 2 mL of dichloromethane and 5 mL of water were added, the samples were mixed vigorously, and the dichloromethane layer was transferred to a new tube. The solution was then completely evaporated under a stream of nitrogen gas, and the prepared sample (1 µL) was injected into a GC with a J&W DB-225 capillary column (30 m × 0.25 mm i.d., 0.25 µm film thickness; Agilent). Helium was used as the carrier gas. The following experimental conditions were used: initial column temperature, 100 °C for 1.5 min followed by a temperature increase of 5 °C/min to 220 °C; injector temperature, 220°C; and flame ionization detector (FID) temperature, 300 °C. There were four biological replications of this experiment.

RESULTS AND DISCUSSION

CAD Cloning

The full-length CAD ortholog in kenaf was cloned using degenerate primers and the RACE system. The sequencing data revealed that the CAD ortholog (GenBank Accession No. KM044582) is composed of a 1,074-bp open reading frame (ORF) encoding 357 amino acids (Fig. 1). The predicted molecular weight of the deduced amino acid sequences, which was calculated using the ExPASy Proteomics Server, is 38.66 kDa, with an isoelectric point (*pI*) of 5.34. According to TargetP1.1 and SignalP 3.0 analysis, the deduced amino acid sequences had no signal for subcellular localization and peptide at the N-terminus, indicating that the CAD protein might be localized in the cytoplasm. A BlastP search showed that the deduced CAD ortholog matched other species of CAD sequences with high similarity (least similarity, 79%), including another, previously reported, kenaf CAD ortholog that matched with 89% similarity. The deduced protein shared the highest similarity, 89%, with *Gossypium hirsutum* (ABZ01817). Multiple alignment revealed that HcCAD contained three conserved motifs in CAD proteins: the Zn₁-binding motif (GHE(X)₂G(X)₅G(X)₂V), the Zn₂-binding motif (GD(X)_{9,10}C(X)₂C(X)₂C(X)₇C), and the NADPH-binding motif (GXG(X)₂G) (Fig. 2) (McKie *et al.* 1993). The Zn₁-binding motif in the deduced protein was located at amino acid residues 68 to 82 and the Zn₂-binding motif was at residues 88 to 114, including the previously identified structural zinc ion coordinating residues (Cys 100, Cys 103, Cys 106, and Cys 114) (Vallee and Aulds 1990). The NADPH-binding motif was placed at residues 188 to 193.

```

atggtagccttgaacccgagagaaaaaacagggtgggcagctagagacccttcaggc 60
  M G S L E T E R K T T G W A A R D P S G

ttcttgcctcttacacgtactctcttaggaacactggtccggaagatgtttcatcaag 120
  F L S P Y T Y S L R N T G P E D V F I K

gttttatttgggatctgccatactgatattcatcaagccaaaaacgatcttggcatg 180
  V L F C G I C H T D I H Q A K N D L G M
                                * * * * *

tccaactcaccatggttctctggacatgaagtgttggtaggtgttggaaataggttca 240
  S N Y P M V P G H E V V G E V L E I G S

gatgtaaccaagtttgcggcggcgaaatcgtcggcgtcgttgccttggtagtggc 300
D V T K F A A G E I V G V G C L V G C C
                                *

aggagtgcaggccaagcaacacagaccgtgagcagctactgtccaagaagatctgtgc 360
R S C R P C N T D R E Q Y C P K K I W S
                                *

tacaacgatgtctacaccgatggcaattccactcaaggtgatttccggttccatgggt 420
  Y N D V Y T D G N S T Q G G F A G S M V

gttgatcaaaaagtttgggtgaagatccagacggaatggcagcggagcagggtggcggc 480
  V D Q K F V V K I P D G M A A E Q V A P

ctgctatgcgccgggatcacagtttacagcccgtgaaccacttcggtttaacggggagt 540
  L L C A G I T V Y S P L N H F G L T G S

ggcttaaggaggaggagtgttgggactcggaggagtagggcacatgggggtaaaatagcc 600
  G L R G G V L G L G G V G H M G V K I A

aaagcaatgggacaccatgtgaccgtcataagctcaaccgacaagaaaaagtcgaggca 660
  K A M G H H V T V I S S S D K K K V E A

ttggagcatctcggcggcagcaataacttagtcagctccgacggcgaagcatgctaaag 720
  L E H L G A D E Y L V S S D A E G M L K

gcccggcaatcgctcgtatatacactcagaccgtgcccgttttccaccctctcgagcct 780
  A A E S L D Y I I D T V P V F H P L E P

tacctttcgttctaactcgtatggaaattgatcttaccggcgttatacaactcct 840
  Y L S L L T L D G K L I L T G V I N T P
                                *

ctccaattccttacacccttgcgtgactcgggaggaagaaatcacagggagtttcat 900
  L Q F L T P L L M L G R K E I T G S F I
                                * * * * *

gggagcatgaagaaacagaggagatgttggcattttgcaagaaaaagattgacatca 960
  G S M K E T E E M L A F C K E K D L T S

atgatcgaagtggtgaaaatgattatgtaaacacagctttggagagcctcagaagaac 1020
  M I E V V K M D Y V N T A L E R L E K N

acgttcgatatcgggtcgtcgtcagcttggcggaaagcaagctcgaatccatag 1074
  D V R Y R F V V D V A G S K L D P

```

Fig. 1. Full-length coding and deduced amino acid sequences of kenaf cinnamyl alcohol dehydrogenase ortholog (HcCAD2). The start codon (ATG) and stop codon (TAG) are underlined and in bold. The conserved residues of CAD are also underlined: (A) Zn₁-binding motif, (B) Zn₂-binding motif, and (C) NADPH-binding motif. Each upper case letter marked by an asterisk (*) indicates a putative substrate binding site.

Superfamily analysis also revealed that the deduced protein contained an expected GroES-like domain at the N-terminus and NAD(P)-binding Rossmann-fold domains at the C-terminus. According to Youn *et al.* (2006), AtCAD5, one of the Arabidopsis CAD proteins, contained a putative substrate-binding pocket composed of the following 12 residues: T⁴⁹, Q⁵³, L⁵⁸, M⁶⁰, C⁹⁵, W¹¹⁹, V²⁷⁶, P²⁸⁶, M²⁸⁹, L²⁹⁰, F²⁹⁹, and I³⁰⁰. When compared to the residues of AtCAD5, the residues of HcCAD1 were different at L⁹⁵, V¹¹⁹, and I²⁹⁰; however, the HcCAD2 residues were exactly the same as the AtCAD5 substrate-binding residues.

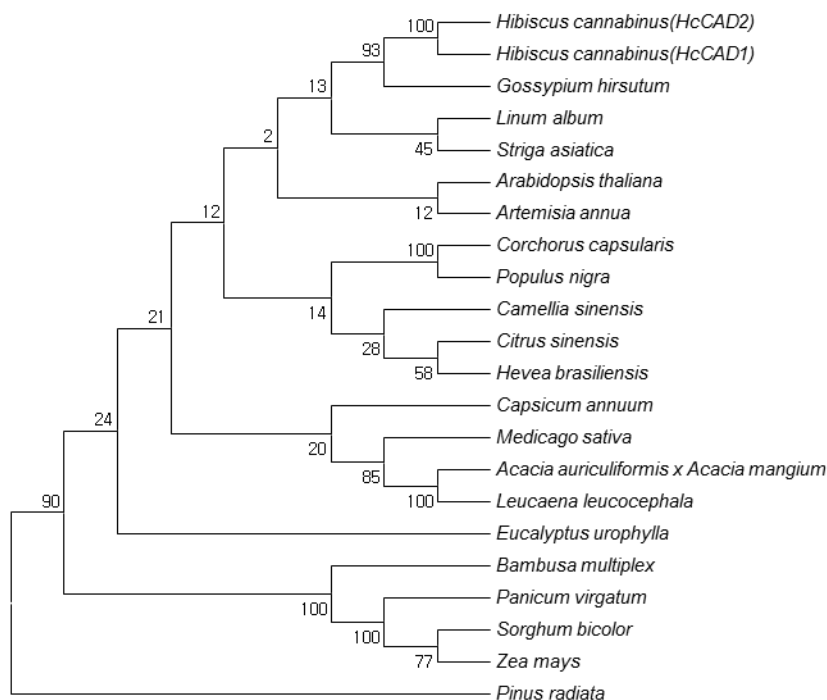


Fig. 3. Phylogenetic tree of the deduced amino acid sequences of CAD proteins from various plants. The phylogenetic tree was designed by the neighbor-joining method of ClustalW and Mega5. The numbers at the nodes indicate bootstrap values from 1,000 replications. The GenBank accession numbers were as follows: *Hibiscus cannabinus* (HcCAD1, ADK24218), *Hibiscus cannabinus* (HcCAD2, KM044582), *Gossypium hirsutum* (ABZ01817), *Linum album* (CAH19074), *Striga asiatica* (ABG35772), *Arabidopsis thaliana* (NP188576), *Artemisia annua* (ACB54931), *Corchorus capsularis* (AAR89392), *Populus nigra* (ADN96375), *Camellia sinensis* (AEE69007), *Citrus sinensis* (ABM67695), *Hevea brasiliensis* (ADU64756), *Capsicum annuum* (ACF17645), *Medicago sativa* (AAL34329), *Acacia auriculiformis* x *Acacia mangium* (ABX75855), *Leucaena leucocephala* (ABJ80682), *Eucalyptus urophylla* (ACU77870), *Bambusa multiplex* (ADG02378), *Panicum virgatum* (ADO01601), *Sorghum bicolor* (BAF42789), *Zea mays* (ACG45271), and *Pinus radiata* (AAC31166)

Analysis of the evolutionary relationship of the CAD ortholog using MEGA5 (Fig. 3) showed that both HcCAD1 and HcCAD2 were closely correlated with *Gossypium hirsutum* (GhCAD1, ABZ01817). GhCAD1 was classified as Class III, having high similarity with *Populus tremuloides* (PtSAD, AAK58693) and AtCAD1 (At4g39330), and was involved in a compensatory mechanism for the biosynthesis of coniferyl alcohol (Bomati and Noel 2005). AtCAD1 was also classified as Class III and catalyzed the reduction of cinnamaldehyde, sinapaldehyde, and coniferaldehyde, as well as several aliphatic aldehydes and various substituted benzaldehydes. GhCAD1 also used sinapaldehyde and coniferaldehyde as substrates for conversion into their corresponding alcohols (Fan *et al.* 2009). Thus, the HcCAD2 protein might have a similar function as GhCAD1 and AtCAD1. Overall, the cloned putative CAD ortholog of kenaf might belong to a CAD enzyme. Hence, CAD was named (ADK24218) *HcCAD1* and (KM044582) *HcCAD2*.

Enzyme Activity of the Recombinant HcCAD2

To characterize the HcCAD2 enzyme activity, recombinant protein was expressed in an *E. coli* system and purified using Ni-TNA resin, after which its catalytic activity toward three probable substrates was examined (Table 1). The highest catalytic characteristics were determined based on the K_m , V_{max} , and K_{enz} (K_{cat}/K_m , the calculated catalytic efficiency) values. The results suggested that HcCAD2 protein had the highest catalytic efficiency (K_{cat}/K_m) toward coniferyl aldehyde and relatively higher efficiency toward sinapyl aldehyde than cinnamyl aldehyde. In other words, preferable substrates of HcCAD2 were coniferyl and sinapyl aldehydes. Although benzyl aldehyde was also tested, no activity was found (data not shown). As expected from phylogenetic analysis, HcCAD2 exhibited a similar preference for substrates as AtCAD1 and GhCAD1. Taken together, these results indicate that HcCAD2 is a *bona fide* CAD enzyme that is prominently involved in the lignin biosynthesis pathway.

Table 1. Kinetic Parameters of the Recombinant HcCAD2 Protein

Substrate	K_m (μM)	V_{max} ($\mu\text{mol}/\text{min}\cdot\text{mg}$)	K_{cat} (1/S)	K_{enz} (1/S·M)
Coniferyl aldehyde	28.17 \pm 6.2	45.96 \pm 3.48	7564.25	26,8512.48
Sinapyl aldehyde	47.1 \pm 14.09	56.92 \pm 7.72	9368.08	198,897.74
Cinnamyl aldehyde	14.25 \pm 4.53	8.73 \pm 1.04	1436.81	100,828.95

Each value calculated using 3 independent replicates; the means \pm standard errors are shown.

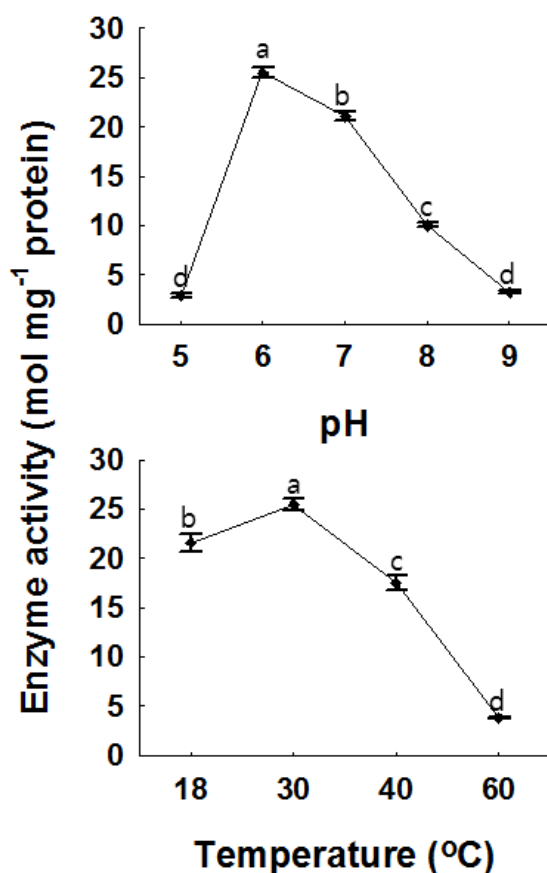


Fig. 4. Effects of pH and temperature on recombinant HcCAD2 activity. Coniferyl aldehyde and NADPH were employed as substrates, and phosphate potassium buffer (200-mM) was used. For the pH assay, the temperature was 30 °C, while the pH was 6.0 for the temperature assay. Prior to the reaction, mixtures were kept in a water bath for 15 min, after which the activity was calculated. Each value indicates the mean \pm standard error based on three independent replications. The letters on each point reveal significant differences between the mean values ($P < 0.05$)

As shown in Fig. 4, the activity of the HcCAD2 enzyme was vulnerable to pH and temperature. HcCAD2 exhibited the highest enzyme activity at pH 6.0, and this level of activity was maintained up to pH 7.0; however, the activity abruptly declined at pH 8.0 and the enzyme appeared to become completely inactive at pH 9.0 and pH 5.0. These results indicate that the activity of the HcCAD2 enzyme is rigorously controlled by pH. According to the optimal pH determined in this study, the enzyme is suitable for cytosolic localization as identified in wheat (Ma 2010). However, contrary to the wheat CAD enzyme, the optimal activity of HcCAD2 was observed at 30 °C. This might have occurred because HcCAD is more stable than wheat CAD enzyme.

Histochemical Analysis of Lignin Distribution during Kenaf Stem Development

Lignin deposition patterns in kenaf stems were observed during developmental stages by staining with phloroglucinol (Fig. 5). The lignin in the stem tissues primarily accumulated in xylem, but not phloem sieve tube cells or parenchyma, in bark. In bark tissues, sclerenchyma fibers were only stained on the outer part of the phloem, indicating that large amounts of lignin were deposited in the tracheary vessels and fibers. Lignin was gradually distributed during the developmental stages in kenaf stem, with high accumulation occurring for up to 4 weeks (Fig. 5A); however, little change was observed from week 4 to 8 (Fig. 5B). Lignin deposition appeared to be completed at 16 to 20 weeks (Figs. 5C and D).

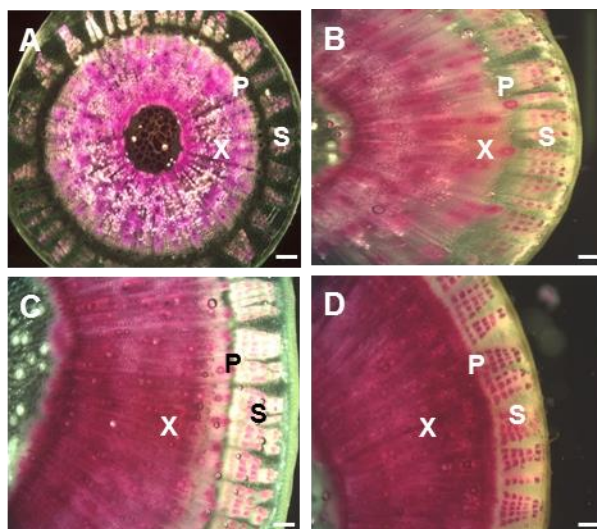


Fig. 5. Histochemical analysis of lignin during developmental stages of kenaf stem. Cross sections of stems were dissected from various aged plants (4, 8, 16, and 20 weeks after sowing). In each stage, lignin deposition was stained by phloroglucine-HCl (red color). (A) 4-week-old stem, (B) 8-week-old stem, (C) 16-week-old stem, and (D) 20-week-old stem. Abbreviations: X, xylem; P, phloem; S, sclerenchyma. Bar = 250 μ m.

Expression Patterns of *Hccad1* and *Hccad2* Transcripts during Developmental Stages and in Various Tissues

For comparative analysis of *HcCAD1* and *HcCAD2* transcripts, expression patterns were investigated during developmental stages and in various tissues (Fig. 6). The transcript levels of *HcCAD1* and *HcCAD2* were highly up-regulated for up to 3 and 4 weeks, respectively. The *HcCAD2* transcript level was much higher than that of *HcCAD1*.

However, the transcript levels of *HcCAD1* and *HcCAD2* sharply declined at weeks 4 and 8, respectively. Although the *HcCAD2* level was recovered to a certain level at week 16 and 20, the *HcCAD1* level did not change significantly (Fig. 6A). These expression patterns were consistent with those of previous studies of the kenaf genes involved in lignin biosynthesis (*HcPAL*, *HcC4H*, *HcCCoAOMT*, *HcHCT*, *HcC3H*, *HcF5H*, *HcCOMT*, and *HcCCR2*) (Choi *et al.* 2012; Chowdhury *et al.* 2012; Ghosh *et al.* 2012; Jeong *et al.* 2012; Chowdhury *et al.* 2013; Kim *et al.* 2013a,b,c; Ghosh *et al.* 2014). As shown in Fig. 5, histochemical analysis revealed that lignin accumulation occurred until week 4 in the stem tissues (data not shown for earlier stages), with no significant change occurring at week 8. These findings are in accordance with the expression patterns of *HcCAD* transcripts. Further lignin accumulation was detected in 16- and 20-week-old stem tissues (Fig. 5). Despite the low expression levels of the transcripts in later stages (8 to 20 weeks), vigorous lignification was detected, possibly due to the cumulative accumulation of lignin and/or posttranslational regulation of the enzyme activity.

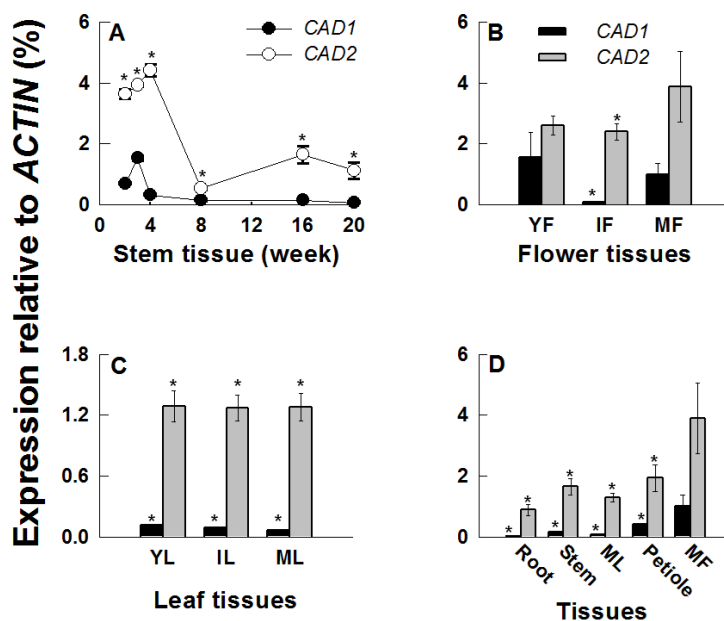


Fig. 6. Expression patterns of kenaf *CAD* orthologs (*HcCAD1* and *HcCAD2*) during developmental stages and in various tissues. The expression levels of *HcCAD1* and *HcCAD2* were measured using Real-time PCR and calculated relative to the *ACTIN* transcript. The expression levels were determined after deduction of the expression level of the control transcript. (A) The expression patterns of *HcCAD1* and *HcCAD2* during stem development (2, 3, 4, 8, 16, and 20 weeks after sowing). (B) The expression patterns of *HcCAD1* and *HcCAD2* during flower development (YF, young flower; IF, immature flower; MF, mature flower). (C) The expression patterns of *HcCAD1* and *HcCAD2* during leaf development (YL, young leaf; IL, immature leaf; ML, mature leaf). (D) The expression patterns of *HcCAD1* and *HcCAD2* in various tissues from 16-week-old plants. Each value indicates the mean \pm standard error based on three biological replications. Probability values between *HcCAD1* and *HcCAD2* expression were determined by a student's t-test. Significant differences ($P < 0.05$) are indicated by an asterisk (*).

The expression of *HcCAD2* in flower tissues was always higher than that of *HcCAD1*, with the highest level occurring in mature flowers (MF) (Fig. 6B). The *HcCAD1* level was highest in young flowers (YF) and lowest in immature flowers (IF). The expression level was consistent during leaf development, with higher levels of *HcCAD2*

than *HcCAD1* occurring (Fig. 6C). The transcript levels of different tissues were measured in 16-week-old plants (Fig. 6D), at which time they were always higher in *HcCAD2* than *HcCAD1*. While the highest levels of the two transcripts were observed in mature flowers (MF), the lowest levels were detected in the roots. Low levels of *HcCAD1* transcript were detected in roots, mature leaves (ML), and stems, indicating that *HcCAD* transcripts play a role in lignifying tissues and generating compounds, which is dependent on the developmental stage and tissue type. In *Arabidopsis*, a considerable amount of phenylpropanoid-derived compounds, including sinapate esters and flavonoids, were accumulated in flower, seed, and silique (Chapple *et al.* 1994). Blanco-Portales *et al.* (2002) reported that in strawberry, *Fxacad1* was expressed in fruit, runners, leaves, and flowers but not in roots, suggesting that the CAD1 enzyme might be associated with the lignification process with regard to both vasculature development and achene maturation. Overall, *HcCAD* transcripts were highly expressed during the early stage of stem elongation and mature stage of flower development and consistently expressed during leaf development.

Expression Patterns of *Hccad1* and *Hccad2* Transcripts under Various Abiotic Stress Conditions

Plants are inevitably subjected to abiotic and biotic stresses throughout their life span. Accordingly, they must develop intracellular defense mechanisms such as changes in gene expression, synthesis of defensive molecules (phytoalexins, phytohormones, and antioxidant enzymes), and lignification for cell-wall reinforcement (Moura *et al.* 2010). Hormone signaling cascade and reactive oxygen species (ROS) signaling pathways are prerequisite to various biotic and abiotic stress responses. In this study, *HcCAD1* and *HcCAD2* expression patterns were studied in 3-week-old seedlings after exposure to MeJA, cold, H₂O₂, SA, ABA, wounding, NaCl, and drought. With the exception of the MeJA and drought treatments, *HcCAD2* was always expressed at higher levels than *HcCAD1* (Fig. 7).

Wound treatment caused the accumulation of *HcCAD1* 1 h after treatment, after which the transcript was reduced to the basal level. *HcCAD2* exhibited the highest induction at 6 h, but was reduced at later times. The transcript level of *HcCAD2* was always higher than that of *HcCAD1*, except at 1 h. Mechanical wounding triggered the induction of genes involved in lignin synthesis, including CAD, leading to lignin deposition around the wound sites (Moura *et al.* 2010). The induction of CAD transcript by wounding has been reported in other plant species (alfalfa, ryegrass, sweet potato) (Brill *et al.* 1999; Lynch *et al.* 2002; Kim *et al.* 2010). *IbCAD1* transcript, classified as a defense-related CAD in sweet potato, was highly upregulated 1 h after wounding and was maintained until 24 h after treatment in root tissues.

In cold treatment, the highest level of the two transcripts was observed at 6 h, with much higher levels being observed in *HcCAD2* than *HcCAD1* (more than fivefold). Two transcripts were reduced at later times. The *HcCAD2* transcript level was always higher than that of *HcCAD1*. Similar expression patterns were reported in *Jatropha curcas* L. (Gao *et al.* 2013). The transcript was significantly up-regulated 5 h after 4 °C chilling treatment. Cold acclimation also induced the genes involved in lignin biosynthesis in soybean and winter barley (Janská *et al.* 2011). Moreover, exposure to extremely low temperatures activated the phenylpropanoid pathway, causing changes in gene expression and metabolites, including lignin (Wei *et al.* 2006).

NaCl treatment highly up-regulated *HcCAD2* at 6 h, while *HcCAD1* expression was not significantly affected by NaCl. The *HcCAD2* transcript level was down-regulated at 12

and 24 h, then up-regulated at 48 h. Sweet potato calli overexpressing *IbLEA14* (*Ipomoea batatas* late embryogenesis abundant 14) showed increased CAD expression when treated with 300-mM NaCl (Park *et al.* 2011). It has been reported that excess salinity in soil stimulates the accumulation of lignin and the alteration of components in the roots of various plants such as soybean, maize, and tomato (Sanchez-Aguayo *et al.* 2004; Neves *et al.* 2010). These results indicate that lignification plays a crucial role in plants' resistance to salt stress.

SA treatment also highly up-regulated *HcCAD2* at 6 h, while no change was observed in *HcCAD1*. Among the various treatments, the highest induction relative to the control was observed in *HcCAD2* at 6 h in response to SA treatment, and the expression patterns were similar to those of NaCl responses. Similar induction was reported in *Linum album*, in which the genes involved in lignin synthesis (*PAL*, *CCR*, and *CAD*) were highly up-regulated 8 to 12 h after SA treatment (Yousefzadi *et al.* 2010).

H₂O₂ treatment caused phenotypic changes (data not shown) with high inductions of both *HcCAD1* and *HcCAD2*. Among the various treatments, the second highest induction relative to the control was observed in *HcCAD2* at 6 h after exposure to H₂O₂. Kim *et al.* (2010) reported that the *IbCAD1* transcript was significantly increased 12 and 24 h after H₂O₂ treatment in sweet potato (Kim *et al.* 2010). Pathogen infection triggered the activation of the phenylpropanoid pathway to fortify cell-wall rigidity, which was correlated with H₂O₂ generation at the infected sites (Kostyn *et al.* 2012). H₂O₂ played a pivotal role in lignin polymerization. Overall, these findings indicate that *HcCADs* may play an indispensable role in defense against pathogen infection with H₂O₂.

ABA treatment induced a biphasic expression pattern of *HcCAD2* transcript with high induction at 6, 24, and 48 h and temporary reduction at 12 h. The induced biphasic expression pattern was also detected in *HcCCoAOMT* with MeJA treatment and *4CL1/4CL2* transcripts in *Arabidopsis thaliana* with wound treatment (Ghosh *et al.* 2012). This biphasic expression pattern suggests that *HcCAD2* is involved in multiple ABA signaling pathways. However, *HcCAD1* was not significantly changed by ABA treatment. It is well-known that ABA is involved in abiotic signal cascades such as those associated with drought and salt stress. In the *IbCAD1* promoter region, phytohormone-binding sites such as ABRE for ABA, ARR for cytokinin, and as-1 element for auxin/SA have been identified (Yokoyama *et al.* 2007). Additionally, *IbCAD1* promoter exhibited increased activity in response to ABA, BA, JA, and SA treatments (Kim *et al.* 2010). The ABA responsive motif was also found in the *Populus* CAD promoter region (Barakat *et al.* 2009). Taken together, these findings suggest that the *CAD* gene is intimately related to ABA signaling.

MeJA treatment generated similar expression patterns in *HcCAD1* and *HcCAD2*, which exhibited high induction at early (1 h) and late time points (48 h) and declination at intermediate time points (6 to 24 h). Sun *et al.* (2013) reported that MeJA treatment stimulated the expression of *CAD1* and *CAD2* transcripts in *Plagiochasma appendiculatum* and that these transcripts played equivalent roles in both lignin biosynthesis and resistance against stresses.

Drought treatment caused higher induction in *HcCAD1* than in *HcCAD2* at all times. *HcCAD1* was highly up-regulated at 14 d, while *HcCAD2* was gradually reduced during treatment. These results indicate that *HcCAD1* is more likely to be involved in the tolerance of water deficiency. The effects of water deficiency on lignin biosynthesis are well known. The aromatic structure of lignin enables plants to prevent transpiration and maintain normal turgor under water-deficient conditions. Inbred maize lines with higher

lignin synthesis had greater drought tolerance with induced expression of *CAD*, *COMT*, and *SAMS* (Hu *et al.* 2009). Similar results have been observed in other plants, such as rice and *Citrullus lanatus* sp. (Yang *et al.* 2006; Yoshimura *et al.* 2008), confirming these findings.

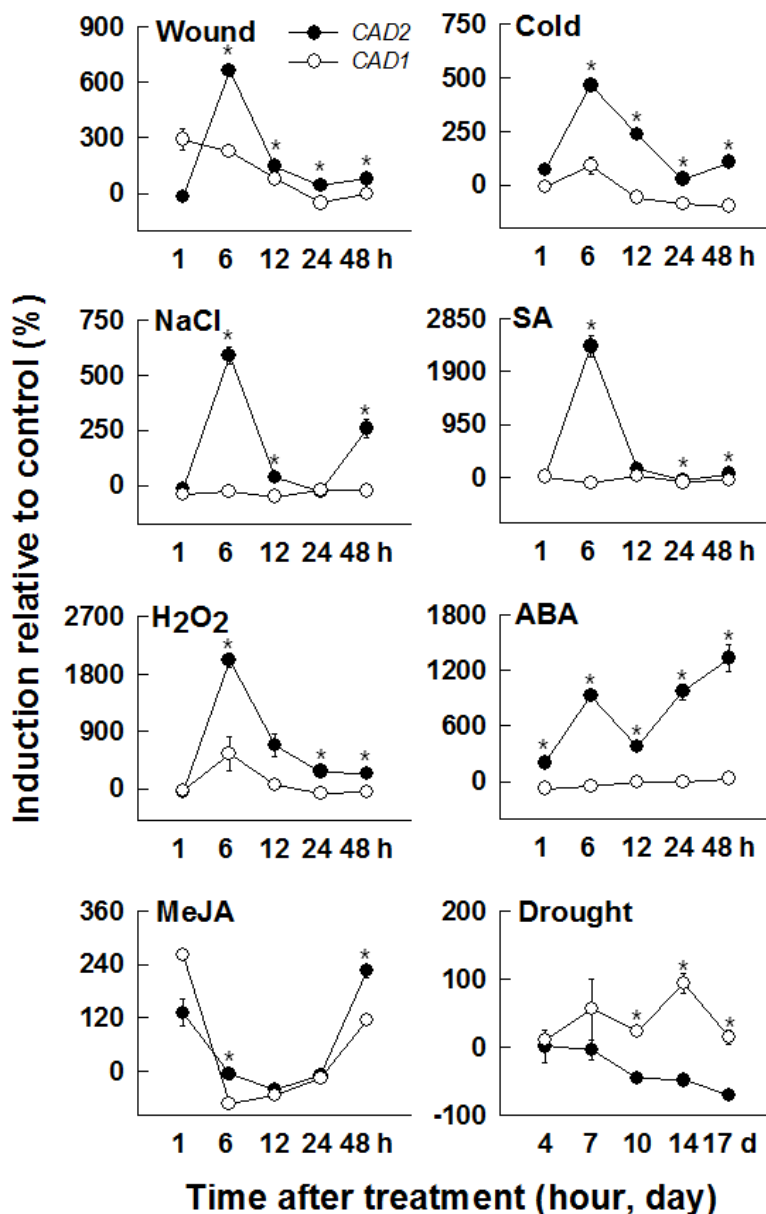


Fig. 7. Expression patterns of kenaf *CAD* orthologs (*HcCAD1* and *HcCAD2*) under diverse stress conditions. Three-week-old kenaf stems were exposed to different treatments [wound, cold, NaCl, salicylic acid (SA), H_2O_2 , abscisic acid (ABA), methyl jasmonate (MeJA), and drought]. The expression levels of *HcCAD1* and *HcCAD2* were measured using QPCR and calculated relative to *ACTIN* transcript. The expression levels were determined after deduction of the expression level of the control transcript. Each value indicates the mean \pm standard error with three biological replications. Probability values between *HcCAD1* and *HcCAD2* expression level were determined by a student's t-test. Significant differences ($P < 0.05$) are indicated by an asterisk (*)

Comprehensive Analysis of Gene Expression Involved in Lignin Biosynthesis during Developmental Stages of the Kenaf Stem

To better understand lignin synthesis during stem development, it is necessary to analyze overall gene expression patterns. Previously reported gene expression patterns are summarized in Fig. 8. During kenaf stem development, every gene involved in lignin synthesis was highly up-regulated for up to four weeks. Among the genes, *HcCCoAOMT* and *HcCOMT* showed the highest expression levels (13- and 32-fold induction relative to kenaf *ACTIN*, respectively), while other genes were up-regulated by 4- to 7-fold.

COMT catalyzes the conversion of both 5-OH-coniferaldehyde and 5-OH coniferyl alcohol to sinapaldehyde and sinapyl alcohol, respectively (Rastogi and Dwivedi 2008). Down-regulation of *COMT* resulted in the reduction of total lignin with a low S/G ratio in tobacco, alfalfa, and maize (Li *et al.* 2008). Thus, the high S/G ratio in kenaf fiber might be attributable to the high *HcCOMT* transcript level. Another reason for these findings might be the substrate preference of HcCAD enzymes, which have high affinity to sinapyl aldehyde and coniferyl aldehyde.

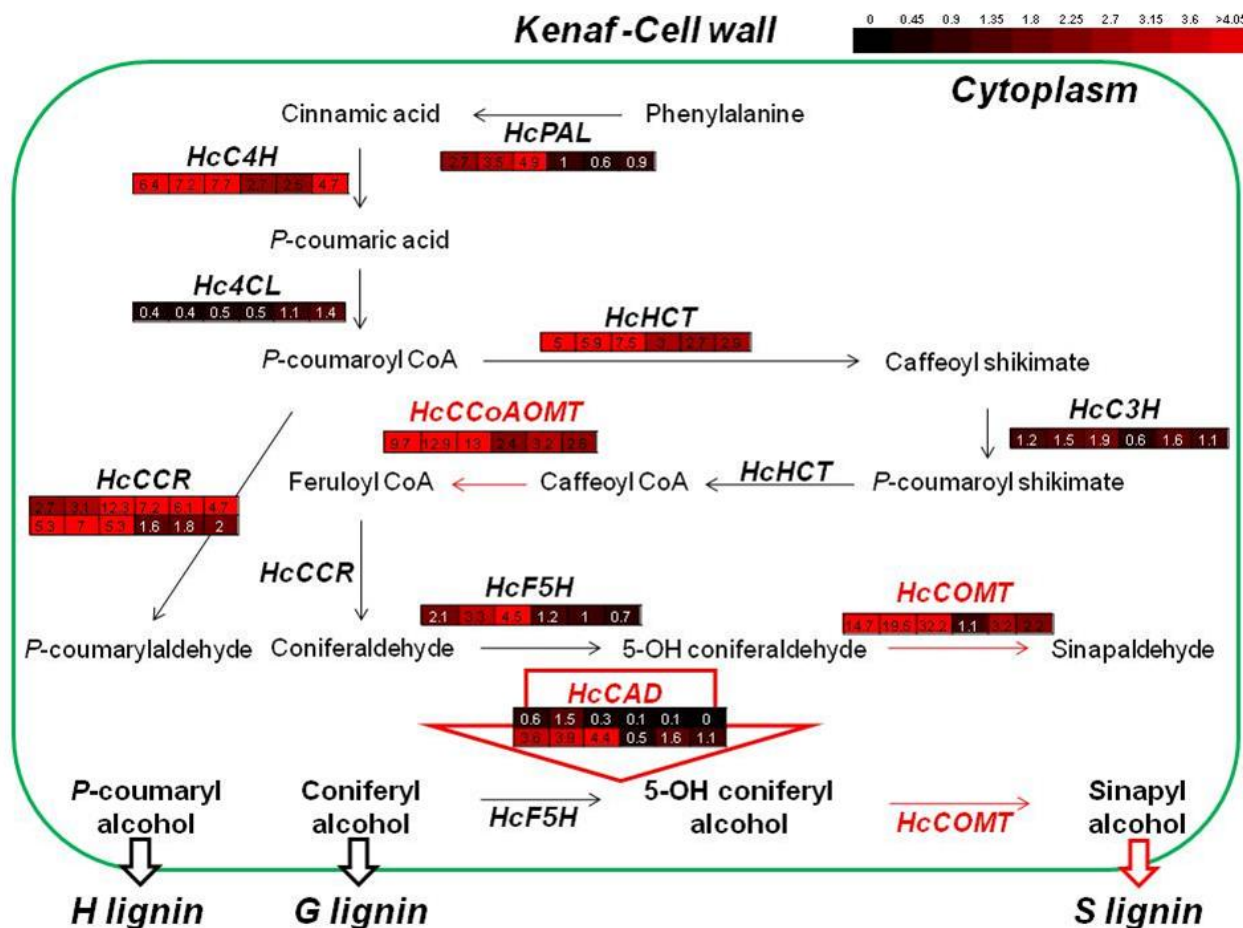


Fig. 8. Comprehensive analysis of gene expression involved in lignin biosynthesis during different developmental stages of kenaf stems. The expression patterns of the genes were previously reported. Each colored box represents the expression level of each gene during different stem developmental stages (2, 3, 4, 8, 16, and 20 weeks after sowing).

Analysis of Composition and Content of Lignin and Sugar during Stem Development

Alkaline nitrobenzene oxidation was applied to characterize the lignin structures in kenaf fibers (Lam *et al.* 2002). Table 2 shows the yield and components of the phenolic acids and aldehydes obtained from alkaline nitrobenzene oxidation of the six alkali-soluble lignins. The most abundant component of the phenolic monomers was syringaldehyde, which was derived from the degradation of non-condensed S units. The second major degradation product, vanillin, was derived from the degradation of non-condensed G units. The S/G ratio gradually increased during stem development, likely due to the large amount of S units in kenaf fibers. These findings indicate that the linear chains of S units are an indispensable portion of the lignin in kenaf fibers. Four phenolic acids, p-hydroxybenzoic acid, syringic acid, p-coumaric acid, and ferulic acid, were also detected in minor quantities.

The composition and content of the associated polysaccharides in kenaf fibers were determined by the neutral sugar contents (Table 3). High levels of sugars were extracted from kenaf fibers, which is consistent with the results of previous studies (Gutiérrez *et al.* 2004). Glucose and xylose were found to be the two major sugars (76.5 and 15.8% of the total sugars, respectively). These results indicate that most chemical bonds between lignin and polysaccharides were cleaved during the alkali treatment processes, which might have been due to the high S/G ratio in kenaf fiber (Table 2). Overall, the results indicate that kenaf fiber is a valuable biomass for use in bioethanol production.

Table 2. Analysis of Phenolic Monomers of Nitrobenzene Oxidation Products of Lignin in Kenaf Stems during Developmental Stages

Week	p-Hydroxybenzoic acid	Vanillin	Syringaldehyde	Syringic acid	p-Coumaric acid	Ferulic acid	S/G ratio
4	0.16 ^c ±0.03	0.60 ^b ±0.05	1.28 ^a ±0.22	0.52 ^b ±0.11	0.16 ^c ±0.01	0.11 ^c ±0.02	3.00±0.22
8	0.12 ^c ±0.04	0.59 ^b ±0.02	1.31 ^a ±0.05	0.61 ^b ±0.17	0.1 ^c ±0.01	0.07 ^c ±0.01	3.23±0.28
16	0.05 ^c ±0.01	0.82 ^b ±0.01	2.37 ^a ±0.15	0.2 ^c ±0.03	0.07 ^c ±0.02	0.2 ^c ±0.06	3.17±0.26
20	0.1 ^d ±0.05	1.03 ^b ±0.05	2.98 ^a ±0.13	0.71 ^{bc} ±0.42	0.07 ^d ±0.01	0.18 ^{cd} ±0.02	3.60±0.36

Each value indicates the mean ± standard error based on four independent replications. p-hydroxybenzaldehyde and vanillic acid were generated in trace amounts and were below the detection limit. Yield (%): weight of lignin monomer/weight of extractives-free samples. S/G ratio: S represents the total yield of syringe aldehyde and syringic acid, G represents the total yield of vanillin and vanillic acid. Different letters indicate significant differences between the mean values ($P < 0.05$).

CONCLUSIONS

1. The results of this study demonstrate that *HcCAD1* and *HcCAD2* are indispensable for lignification in various tissues, as well as for defending plants under diverse stress conditions.

2. The expression of *HcCADs* with other genes involved in lignin synthesis can be attributed to condensation of high levels of S lignin during kenaf stem development.
3. High levels of usable sugars can be extracted from kenaf fibers, demonstrating the potential for using kenaf fibers as a valuable biomass source for bioethanol production.

ACKNOWLEDGMENTS

This research was supported by the Yeungnam University Research Grant in 214A367017.

REFERENCES CITED

- Bae, H., Kim, S.-H., Kim, M. S., Sicher, R. C., Strem, M. D., Natarajan, S., and Bailey, B. A. (2008). "The drought response of *Theobroma cacao* (cacao) and the regulation of genes involved in polyamine biosynthesis by drought and other stresses," *Plant Physiol. Bioch.* 46(2), 174-188. DOI: 10.1016/j.plaphy.2007.10.014
- Barakat, A., Bagniewska-Zadworna, A., Choi, A., Plakkat, U., DiLoreto, D. S., Yellanki, P., and Carlson, J. E. (2009). "The cinnamyl alcohol dehydrogenase gene family in *Populus*: Phylogeny, organization, and expression," *BMC Plant Biol.* 9(26), DOI: 10.1186/1471-2229-9-26
- Blanco-Portales, R., Medina-Escobar, N., Lopez-Raez, J. A., Gonzalez-Reyes, J. A., Villalba, J. M., Moyano, E., Caballero, J. L., and Munoz-Blanco, J. (2002). "Cloning, expression and immunolocalization pattern of a *cinnamyl alcohol dehydrogenase* gene from strawberry," *J. Exp. Bot.* 53(375), 1723-1734. DOI: 10.1093/jxb/erf029
- Bomati, E. K., and Noel, J. P. (2005). "Structural and kinetic basis for substrate selectivity in *Populus tremuloides* sinapyl alcohol dehydrogenase," *Plant Cell.* 17(5), 1598-1611. DOI: 10.1105/tpc.104.029983
- Brill, E. M., Abrahams, S., Hayes, C. M., Jenkins, C. L. D., and Watson, J. M. (1999). "Molecular characterisation and expression of a wound-inducible cDNA encoding a novel cinnamyl-alcohol dehydrogenase enzyme in Lucerne (*Medicago sativa* L.)," *Plant Mol. Biol.* 41(2), 279-291. DOI: 10.1023/A:1006381630494
- Chapple, C. C. S., Shirley, B. W., Zook, M., Hammerschmidt, R., and Somerville, S. C. (1994). "Secondary metabolism in *Arabidopsis*," in: *Arabidopsis*, E. M. Meyerowitz (ed.), Cold Spring Harbor Laboratory Press, Cold Spring Harbor, NY, pp. 989-1030.
- Chen, C.-L. (1992). "Nitrobenzen and cupric oxide oxidations," in: *Methods in Lignin Chemistry*, Lin, S. Y., and Dence, C. W. (eds.), Springer, Berlin, pp. 301-321. DOI: 10.1007/978-3-642-74065-7_21
- Choi, B., Kang, S.-Y., Bae, H.-J., Lim, H.-S., Bang, W.-S., and Bae, H. (2012). "Transcriptional analysis of the *p-coumarate 3-hydroxylase* (*C3H*) gene from *Hibiscus cannabinus* L. during developmental stages in various tissues as well as in response to abiotic stresses," *Res. J. Biotech.* 7(3), 23-33.
- Chowdhury, E. M., Choi, B. S., Park, S. U., Lim, H.-S., and Bae, H. (2012). "Transcriptional analysis of *hydroxycinnamoyl transferase* (*HCT*) in various tissues of *Hibiscus cannabinus* in response to abiotic stress conditions," *Plant Omics* 5(3), 305-313.

- Chowdhury, M. E. K., Choi, B., Cho, B.-K., Kim, J. B., Park, S. U., Natarajan, S., Lim, H. S., and Bae, H. (2013). "Regulation of *4CL*, encoding 4-coumarate: coenzyme A ligase, expression in kenaf under diverse stress conditions," *Plant Omics* 6(4), 254-262.
- Dempsey, J. M. (1975). *Fiber Crops*, The University Presses of Gainesville, Gainesville, FL.
- Fan, L., Shi, W.-J., Hu, W.-R., Hao, X.-Y., Wang, D.-M., Yuan, H., and Yan, H.-Y. (2009). "Molecular and biochemical evidence for phenylpropanoid synthesis and presence of wall-linked phenolics in cotton fibers," *J. Integr. Plant Biol.* 51(7), 626-637. DOI: 10.1111/j.1744-7909.2009.00840.x
- Galliano, H., Cabane, M., Eckerskorn, C., Lottspeich, F., Sandermann, H., and Ernst, D. (1993). "Molecular cloning, sequence analysis, and elicitor-/ozone-induced accumulation of cinnamyl alcohol dehydrogenase from Norway spruce (*Picea abies*)," *Plant. Mol. Biol.* 23(1), 145-156. DOI: 10.1007/BF00021427
- Gao, J., Jiang, N., Qin, X., Zhu, X., Ai, T., Peng, T., Peng, T., Wu, J., Wu, Y., and Chen, F. (2013). "Physiological and metabolic responses of *Jatropha* to chilling stress," *Int. J. Agric. Biol.* 15(5), 871-877.
- Ghosh, R., Choi, B., Jeong, M.-J., Bae, D. W., Shin, S. C., Park, S. U., Lim, H.-S., Kim, J., and Bae, H. (2012). "Comparative transcriptional analysis of caffeoyl-coenzyme A 3-O-methyltransferase from *Hibiscus cannabinus* L., during developmental stages in various tissues and stress regulation," *Plant Omics* 5(2), 184-193.
- Ghosh, R., Choi, B., Cho, B.-K., Lim, H.-S., Park, S.-U., Bae, H.-J., Natarajan, S., and Bae, H. (2014). "Characterization of developmental- and stress-mediated expression of *Cinnamoyl-CoA Reductase* in kenaf (*Hibiscus cannabinus* L.)," *Sci. World J.* 2014, 601845. DOI: 10.1155/2014/601845
- Gutiérrez, A., Rodríguez, I., and Del Río, J. (2004). "Chemical characterization of lignin and lipid fractions in kenaf bast fibers used for manufacturing high-quality papers," *J. Agri. Food Chem.* 52(15), 4764-4773. DOI: 10.1021/jf049540w
- Hu, Y., Li, W. C., Xu, Y. Q., Li, G. J., Liao, Y., and Fu, F. L. (2009). "Differential expression of candidate genes for lignin biosynthesis under drought stress in maize leaves," *J. Appl. Genet.* 50(3), 213-223. DOI: 10.1007/BF03195675
- Janská, A., Aprile, A., Zámecník, J., Cattivelli, L., and Ovesná, J. (2011). "Transcriptional responses of winter barley to cold indicate nucleosome remodelling as a specific feature of crown tissues," *Funct. Integr. Genomic.* 11(2), 307-325. DOI: 10.1007/s10142-011-0213-8
- Jeong, M.-J., Choi, B. S., Bae, D. W., Shin, S. S., Park, S. U., Lim, H.-S., Kim, J., Kim, J. B., Cho, B.-K., and Bae, H. (2012). "Differential expression of kenaf phenylalanine ammonia-lyase (*PAL*) ortholog during developmental stages and in response to abiotic stresses," *Plant Omics* 5(4), 392-399.
- Kim, S. J., Kim, M. R., Bedgar, D., Moinuddin, S. G. A., Cardenas, C. L., Davin, L. B., Kang, C. C. K., and Lewis, N. G. (2004). "Functional reclassification of the putative cinnamyl alcohol dehydrogenase multigene family in *Arabidopsis*," *Proc. Natl. Acad. Sci. USA* 101(6), 1455-1460. DOI: 10.1073/pnas.0307987100

- Kim, Y.-H., Bae, J. M., and Huh, G.-H. (2010). "Transcriptional regulation of the cinnamyl alcohol dehydrogenase gene from sweet potato in response to plant developmental stage and environmental stress," *Plant Cell Rep.* 29(7), 779-791. DOI: 10.1007/s00299-010-0864-2
- Kim, J., Choi, B., Cho, B.-K., Lim, H.-Y., Kim, J. B., Natarajan, S., Kwak, E., and Bae, H. (2013a). "Molecular cloning, characterization and expression of the caffeic acid O-methyltransferase (*COMT*) ortholog from kenaf (*Hibiscus cannabinus*)," *Plant Omics* 6(4), 246-253.
- Kim, J., Choi, B., Natarajan, S., and Bae, H. (2013b). "Expression analysis of *kenaf cinnamate 4-hydroxylase (C4H)* ortholog during developmental and stress responses," *Plant Omics* 6(1), 65-72.
- Kim, J., Choi, B., Park, Y.-H., Cho, B.-K., Lim, H.-S., Natarajan, S., Park, S.-U., and Bae, H. (2013c). "Molecular characterization of *Ferulate 5-Hydroxylase* gene from kenaf (*Hibiscus cannabinus* L.)," *Sci. World J.* 2013, 421578. DOI: 10.1155/2013/421578
- Kostyn, K., Czemplik, M., Kulma, A., Bortniczuk, M., Skała, J., and Szopa, J. (2012). "Genes of phenylpropanoid pathway are activated in early response to *Fusarium* attack in flax plants," *Plant Sci.* 190, 103-115. DOI: 10.1016/j.plantsci.2012.03.011
- Lam, T. B. T., Hori, K., and Iiyama, K. (2002). "Structural characteristics of cell walls of kenaf (*Hibiscus cannabinus* L.) and fixation of carbon dioxide," *J. Wood. Sci.* 49, 255-261. DOI: 10.1007/s10086-002-0469-7
- Lapierre, C., Pilate, G., Pollet, B., Mila, I., Leple, J. C., Jouanin, L., Kim, H., and Ralph, J. (2004). "Signatures of cinnamyl alcohol dehydrogenase deficiency in poplar lignins," *Phytochem.* 65(3), 313-321. DOI: 10.1016/j.phytochem.2003.11.007
- Li, X., Weng, J., and Chapple, C. (2008). "Improvement of biomass through lignin modification," *Plant J.* 54(4), 569-581. DOI: 10.1111/j.1365-313X.2008.03457.x
- Lynch, D., Lidgett, A., McInnes, R., Huxley, H., Jones, E., and Mahoney, N. (2002). "Isolation and characterization of three cinnamyl alcohol dehydrogenase homologue cDNAs from perennial ryegrass (*Lolium perenne* L.)," *J. Plant Physiol.* 159(6), 653-660
- Ma, Q.-H. (2010). "Functional analysis of a cinnamyl alcohol dehydrogenase involved in lignin biosynthesis in wheat," *J. Exp. Bot.* 61(10), 2735. DOI: 10.1093/jxb/erq107
- McKie, J. H., Jaouhari, R., Douglas, K. T., Goffner, D., Feuillet, C., Grima-Pettenati, J., Boudet, A. M., Baltas, M., and Gorrichon, L. (1993). "A molecular model for cinnamyl alcohol dehydrogenase, a plant aromatic alcohol dehydrogenase involved in lignification," *Biochim. Biophys. Acta.* 1202(1), 61-69. DOI: 10.1016/0167-4838(93)90063-W
- Moura, J. C., Bonine, C. A., de Oliveira Fernandes Viana, J., Dornelas, M. C., and Mazzafera, P. (2010). "Abiotic and biotic stresses and changes in the lignin content and composition in plants," *J. Integr. Plant Biol.* 52(4), 360-376. DOI: 10.1111/j.1744-7909.2010.00892.x
- Neves, G. Y. S., Marchiosi, R., Ferrarese, M. L. L., Siqueira-Soares, R. C., and Ferrarese-Filho, O. (2010). "Root growth inhibition and lignifications induced by salt stress in soybean," *J. Agron. Crop Sci.* 196(6), 467-473. DOI: 10.1111/j.1439-037X.2010.00432.x
- Pande, H., and Roy, D. N. (1996). "Delignification kinetics of soda pulping of kenaf," *J. Wood. Chem. Technol.* 16(3), 311-325. DOI: 10.1080/02773819608545811

- Park, S. C., Kim, Y. H., Jeong, J. C., Kim, C. Y., Lee, H. S., Bang, J. W., and Kwak, S. S. (2011). "Sweet potato late embryogenesis abundant 14 (*IbLEA14*) gene influences lignification and increases osmotic- and salt stress-tolerance of transgenic calli," *Planta* 233(3), 621-634.
- Ralph, J., Lapierre, C., Marita, J. M., Kim, H., Lu, F., Hatfield, R. D., Ralph, S., Chapple, C., Franke, R., Hemm, M. R., *et al.* (2001). "Elucidation of new structures in lignins of CAD- and COMT-deficient plants by NMR," *Phytochem.* 57(6), 993-1003. DOI: 10.1016/S0031-9422(01)00109-1
- Rastogi, S., and Dwivedi, U. (2008). "Manipulation of lignin in plants with special reference to O-methyltransferase," *Plant Sci.* 174(3), 264-77. DOI: 10.1016/j.plantsci.2007.11.014
- Sanchez-Aguayo, I., Rodriguez-Galan, J. M., Garcia, R., Torreblanca, J., and Pardo, J. M. (2004). "Salt stress enhances xylem development and expression of S-adenosyl-L-methionine synthase in lignifying tissue of tomato plants," *Planta* 220(2), 278-285. DOI: 10.1007/s00425-004-1350-2
- Sun, Y., Wu, Y., Zhao, Y., Han, X., Lou, H., and Cheng, A. (2013). "Molecular cloning and biochemical characterization of two cinnamyl alcohol dehydrogenases from a liverwort *Plagiochasma appendiculatum*," *Plant Physiol. Biochem.* 70, 133-141. DOI: 10.1016/j.plaphy.2013.05.027
- TAPPI (1992). "TAPPI Test Methods," TAPPI Press, Atlanta, GA.
- Vallee, B. L., and Aulds, D. S. (1990). "Zinc coordination, function and structure of zinc enzymes and other proteins," *Biochem.* 29(24), 5647-5659. DOI: 10.1021/bi00476a001
- Wei, H., Dhanaraj, A. L., Arora, R., Rowland, L. J., Fu, Y., and Sun, L. I. (2006). "Identification of cold acclimation-responsive *Rhododendron* genes for lipid metabolism, membrane transport and lignin biosynthesis: importance of moderately abundant ESTs in genomic studies," *Plant Cell Environ.* 29(24), 558-570. DOI: 10.1111/j.1365-3040.2005.01432.x
- Wi, S. G., Kim, H. J., Mahadevan, S. A., Yang, D. J., and Bae, H. J. (2009). "The potential value of the seaweed Ceylon moss (*Gelidium amansii*) as an alternative bioenergy resource," *Bioresour. Technol.* 100(24), 6658-6660. DOI: 10.1016/j.biortech.2009.07.017
- Yang, L., Wang, C. C., Guo, W. D., Li, X. B., Lu, M., and Yu, C. L. (2006). "Differential expression of cell wall related genes in the elongation zone of rice roots under water deficit," *Rus. J. Plant Physiol.* 53(3), 390-395. DOI: 10.1134/S1021443706030150
- Yokoyama, A., Yamashino, T., Amano, Y. I., Tajima, Y., Imamura, A., Sakakibara, H., and Mizuno, T. (2007). "Type-B ARR transcription factors, ARR10 and ARR12, are implicated in cytokinin-mediated regulation of protoxylem differentiation in roots of *Arabidopsis thaliana*," *Plant Cell Physiol.* 48(1), 84-96. DOI: 10.1093/pcp/pcp040
- Yoshimura, K., Masuda, A., Kuwano, M., Yokota, A., and Akashi, K. (2008). "Programmed proteome response for drought avoidance/tolerance in the root of a C-3 xerophyte (wild watermelon) under water deficits," *Plant Cell Physiol.* 49(2), 226-241. DOI: 10.1093/pcp/pcm180

- Youn, B., Camacho, R., Moinuddin, S.G.A., Lee, C., Davin, L. B., Lewis, N. G., and Kang, C. (2006). "Crystal structures and catalytic mechanism of the *Arabidopsis* cinnamyl alcohol dehydrogenases AtCAD5 and AtCAD4," *Org. Biomol. Chem.* 4, 1687-1697. DOI: 10.1039/b601672c
- Yousefzadi, M., Sharifi, M., Behmanesh, M., Ghasempour, A., Moyano, E., and Palazon, J. (2010). "Salicylic acid improves podophyllotoxin production in cell cultures of *Linum album* by increasing the expression of genes related with its biosynthesis," *Biotechnol. Lett.* 32(11), 1739-1743. DOI: 10.1007/s10529-010-0343-4

Article submitted: June 10, 2015; Peer review completed: July 2, 2015; Revisions received: October 21, 2015; Revisions accepted: October 24, 2015; Published: November 9, 2015.

DOI: 10.15376/biores.11.1.105-125